Research Article

Involvement of circRNA Regulators MBNL1 and QKI in the Progression of Esophageal Squamous Cell Carcinoma

Cancer Control
Volume 31: 1–15

DOI: 10.1177/10732748241257142
journals.sagepub.com/home/ccx
Sage

Hai-Feng Wang[1,2], Xiao-Feng Zhou[3], Qun-Mei Zhang[4], Jie-Qing Wu[2], Jing-Han Hou[3], Xue-Lian Xu[2], Xiu-Min Li[3], and Yu-Long Liu[1,5,6]

Abstract

Objectives: To investigate the role of circRNA regulators MBNL1 and QKI in the progression of esophageal squamous cell carcinoma.

Background: MBNL1 and QKI are pivotal regulators of pre-mRNA alternative splicing, crucial for controlling circRNA production – an emerging biomarker and functional regulator of tumor progression. Despite their recognized roles, their involvement in ESCC progression remains unexplored.

Methods: The expression levels of MBNL1 and QKI were examined in 28 tissue pairs from ESCC and adjacent normal tissues using data from the GEO database. Additionally, a total of 151 ESCC tissue samples, from stage T1 to T4, consisting of 13, 43, 87, and 8 cases per stage, respectively, were utilized for immunohistochemical (IHC) analysis. RNA sequencing was utilized to examine the expression profiles of circRNAs, lncRNAs, and mRNAs across 3 normal tissues, 3 ESCC tissues, and 3 pairs of KYSE150 cells in both wildtype (WT) and those with MBNL1 or QKI knockouts. Transwell, colony formation, and subcutaneous tumorigenesis assays assessed the impact of MBNL1 or QKI knockout on ESCC cell migration, invasion, and proliferation.

Results: ESCC onset significantly altered MBNL1 and QKI expression levels, influencing diverse RNA species. Elevated MBNL1 or QKI expression correlated with patient age or tumor invasion depth, respectively. MBNL1 or QKI knockout markedly enhanced cancer cell migration, invasion, proliferation, and tumor growth. Moreover, the absence of either MBNL1 or QKI modulated the expression profiles of multiple circRNAs, causing extensive downstream alterations in the expression of numerous lncRNAs and mRNAs. While the functions of circRNA and lncRNA among the top 20 differentially expressed genes remain unclear, mRNAs like SLCO4C1, TMPRSS15, and MAGEB2 have reported associations with tumor progression.

[1]Department of Oncology, The Second Affiliated Hospital of Soochow University, Suzhou, Jiangsu, China
[2]Department of Oncology, The First Affiliated Hospital of Xinxiang Medical University, Xinxiang, Henan, China
[3]Henan Key Laboratory of Tumor Molecular Therapy Medicine, The Third Affiliated Hospital of Xinxiang Medical University, Xinxiang, Henan, China
[4]Department of Blood Transfusion, The First Affiliated Hospital of Xinxiang Medical University, Xinxiang, Henan, China
[5]State Key Laboratory of Radiation Medicine and Protection, School of Radiation Medicine and Protection, Soochow University, Suzhou, Jiangsu, China
[6]Collaborative Innovation Center of Radiological Medicine of Jiangsu Higher Education Institutions, Suzhou, Jiangsu, P.R. China

Corresponding Authors:
Yu-Long Liu, Department of Oncology, The Second Affiliated Hospital of Soochow University, 1055 Sanxiang Road, Gusu District, Suzhou, Jiangsu 215004, China.
Email: yulongliu2002@suda.edu.cn

Xiu-Min Li, Henan Key Laboratory of Tumor Molecular Therapy Medicine, The Third Affiliated Hospital of Xinxiang Medical University, No. 83, East Section of Hualan Avenue, Hongqi District, Xinxiang, Henan 453003, China.
Email: lxm3029981@126.com

Conclusions: This study underscores the tumor-suppressive roles of MBNL1 and QKI in ESCC, proposing them as potential biomarkers and therapeutic targets for ESCC diagnosis and treatment.

Keywords
ESCC, MBNL1, QKI, circRNA, tumor progression

Received November 27, 2023. Received revised April 25, 2024. Accepted for publication May 3, 2024.

Introduction

According to global cancer statistics in 2020, esophageal cancer (EC) stands as the ninth most common malignancy and ranks sixth among the leading causes of cancer-related deaths.[1] The global incidence of new EC cases reached 604 000, resulting in 544 000 deaths.[1] Particularly, China is a high-incidence region for EC, where despite declining incidence and mortality rates, it remains a prominent malignancy posing a threat to the health of Chinese residents. Histologically, EC is categorized into 2 major subtypes: ESCC and esophageal adenocarcinoma (EAC).[2] ESCC constitutes the most prevalent type globally, accounting for approximately 85% of all cases.[3,4]

Previous research has demonstrated that alterations in the expression levels of tumor suppressors or oncoproteins contribute to the progression of ESCC.[5-10] Notably, Muscleblind-like 1 (MBNL1) is significantly downregulated in various cancers, such as gastric cancer, breast cancer, glioma, and leukemia.[11] Similarly, changes in the expression of the quaking (QKI) protein have been observed in lung, colon, gastric, and prostate cancer.[12-15] Numerous studies have proposed that both MBNL1 and QKI function as tumor suppressors in specific cancers.[16,17] Interestingly, MBNL1 and QKI are recognized as crucial pre-mRNA alternative splicing regulators[18] and play a key role in splicing alterations observed in various human solid tumors.[12,19] As RNA binding proteins (RBPs), MBNL1 and QKI exhibit both positive and negative regulatory effects on circRNA production,[20] with alterations in circRNA levels implicated in either promoting or suppressing cancer progression.[21] However, the expression patterns of MBNL1 and QKI in the clinical pathology of ESCC and their roles in regulating circRNA production in ESCC require further investigation.

In this study, we investigated the role of MBNL1 and QKI in ESCC, focusing on their impact on circRNA production and their involvement in influencing cancerous growth. Our findings unveil a novel molecular mechanism through which MBNL1 and QKI-mediated circRNA production regulates ESCC growth.

Methods

Bioinformatics Analysis

The GSE161533 dataset acquired from the GEO database was utilized to assess the expression levels of MBNL1 and QKI throughout ESCC tissues and adjacent normal tissues isolated from cancer patients. Kaplan-Meier survival analysis was utilized to assess the correlation between the expression levels of MBNL1 or QKI and the survival prognosis of cancer patients.

Tissue Microarray (TMA) and IHC

A comprehensive assembly of 151 ESCC tissue samples, from stages T1 to T4, distributed with 13, 43, 87, and 8 cases per stage, respectively, were employed to construct a TMA. The Ethics Committee of the First Affiliated Hospital of Xinxiang Medical University approved the clinical ESCC samples used in this study (ethics approval number: 2018390). In esophageal carcinoma, postoperative pathological assessment of surgical specimens allows for the stratification of tumor invasion depth into stages T1 through T4. Stage T1 is characterized by tumor invasion in the mucosal sublayer, the muscularis mucosae, or the submucosa of the esophagus. Stage T2 suggests deeper invasion reaching the muscularis propria, a robust muscle layer in the esophageal wall. Stage T3 is defined by tumor penetration into the adventitia, the outermost tissue layer of the esophageal wall. Stage T4 is characterized by tumor extension into adjacent structures, including the pleura, pericardium, major blood vessels, diaphragm, or peritoneum, as well as the aorta, vertebrae, or trachea. Notably, none of the recruited patients were administered preoperative treatments, reducing potential confounding effects on the results. Standard IHC was conducted, and IHC scores were determined with the following formula: IHC score = intensity score × percentage score. The intensity score was assessed according to the staining intensity (0 = negative, 1 = weak, 2 = moderate, and 3 = strong). The percentage score was determined using the percentage of stained area (0 = 0%, 1 = 1%-25%, 2 = 26%-50%, 3 = 51%-75%, and 4 = 76%-100%). According to the IHC score, samples were categorized into a low-QKI (or MBNL1) expression group (IHC score <6) or a high-QKI (or MBNL1) expression group (IHC score ≥6).

Cell Culture

The human esophageal carcinoma cell line, KYSE150, was acquired from Procell Life Science & Technology. These cells

were grown using RPMI 1640 medium (Gibco, Thermo Fisher Scientific, Waltham, MA, USA) supplemented with 10 % fetal bovine serum (FBS, Pan-Biotech, Aidenbach, Germany) and 1 × penicillin/streptomycin (Invitrogen). The cell culture was maintained in a humidified incubator at 37°C and a 5 % CO_2 atmosphere.

Generation of MBNL1$^{-/-}$ and QKI$^{-/-}$ Cell Lines

Following previously established research protocols,[22] 3 sgRNAs targeting MBNL1 or QKI genes were designed using an online tool (https://crispor.tefor.net/). Thereafter, sgRNA primers were synthesized, annealed, and successively cloned into the pX458-ECFP and pX458-DsRed2 vectors. KYSE150 cells were electroporated with the 3 plasmids possessing the sgRNA using the Nucleofector™ 2b Device (Lonza). Following the transfection (48 hours later), ECFP and DsRed2 double-positive cells were obtained through flow cytometry, and these sorted cells were cultured for an additional 14 days to allow for expansion. Verification of the knockout was performed via PCR amplification, agarose gel electrophoresis, DNA sequencing, and quantitative real-time PCR (qRT-PCR). The sequences of the sgRNA and PCR primers for MBNL1 and QKI are outlined in Supplemental Figure 1.

Total RNA Extraction and RNA Sequencing Analysis

Total RNA was isolated using TRIzol reagent (Invitrogen, Carlsbad, CA, USA) from 3 pairs of normal and tumor tissue samples extracted from patients, alongside 3 sets of WT and either MBNL1-or QKI-deficient cell lines. Total RNA was then assayed for quality and quantity with a NanoDrop and an Agilent 2100 bioanalyzer (Thermo Fisher Scientific, MA, USA). The total RNA library was constructed, and paired-end sequencing was performed using the MGISEQ-2000 System (BGI-Shenzhen, China). The sequencing data was refined using SOAPnuke (v1.5.2),[23] and the clean reads were mapped to the reference genome utilizing HISAT2 (v2.0.4).[24] Bowtie2 (v2.2.5) was employed to align the clean reads to a reference gene set[25] in a database compiled by the Beijing Genomic Institute in Shenzhen, incorporating known and novel coding and noncoding transcripts. The expression levels of each gene were calculated using RSEM (v1.2.12),[26] and a heatmap was developed using Pheatmap (v1.0.8). Differential expression analysis was performed using DESeq2 (v1.4.5) with a stringent cutoff (q-value ≤.05),[27] and the levels of significance were corrected using the q-value. The raw data were submitted to the CNGB database (Submission number: sub038716, Project number: CNP0003791, https://db.cngb.org/).

qRT-PCR

Total RNA was isolated from ESCC tumor tissues and adjacent normal tissues, alongside WT and gene knockout KYSE150 cell lines, utilizing TRIzol reagent (Invitrogen, Carlsbad, CA, USA). The RevertAid First Strand cDNA Synthesis Kit (Thermo Fisher Scientific, MA, USA) was utilized for cDNA synthesis. Individual qRT-PCR reactions were performed to quantify MBNL1 and QKI expression levels in WT and knockout cell lines, as well as to validate the expression levels of overlapping differentially expressed genes characterized via RNA sequencing. The primer sequences employed for qRT-PCR can be found in Supplemental Table 1.

Western Blotting

To confirm the successful knockout of MBNL1 or QKI at the protein level in KYSE150 cells, we performed western blotting. Initially, WT and MBNL1$^{-/-}$ or QKI$^{-/-}$ KYSE150 cells were harvested and lysed using RIPA lysis buffer (Beyotime, Shanghai, China) supplemented protease inhibitor (1:100, NCM Biotech, Suzhou, China) on ice for 30 minutes to isolate proteins. Protein samples were integrated with 5 × loading buffer (4:1) and heated to 100°C for 10 minutes. The samples were separated using SDS-PAGE and transferred to a PVDF membrane. Following blocking with 10 % skimmed milk powder, the membrane was incubated with primary antibodies targeting MBNL1 (YN8753, Immunoway, 1:2000), QKI (YT7323, Immunoway, 1:2000), and HSP90 (YT5327, Immunoway, 1:2000). Following incubation, the membrane was rinsed 5 times with 1 × TBST and incubated with a goat anti-rabbit secondary antibody. After 5 additional 1 × TBST washes, the detection was carried out using a chemiluminescent HRP substrate (Millipore) and imaged using an automatic chemiluminescence image analysis system (Tanon-5200).

Transwell and Colony Formation Assays

Transwell and colony formation assays were conducted as previously outlined.[28] Specifically, for migration assays, the WT and MBNL1$^{-/-}$ or QKI$^{-/-}$ KYSE150 cells in serum-free RPMI 1640 medium were placed into the upper chambers. For invasion assays, Matrigel (BD Biocoat, USA) was applied to coat the upper chambers. After coating, the WT and MBNL1$^{-/-}$ or QKI$^{-/-}$ KYSE150 cells in serum-free medium were placed into the Matrigel-coated upper chambers. After 24 hours, the cells that migrated to the bottom of the membrane were fixed using 4 % paraformaldehyde, stained with crystal violet, and totaled under a microscope with a 20 × objective lens.

For colony formation assays, cells were placed into 12-well plates containing 500 cells per well for 2 weeks. After removal of the medium, cells were rinsed 3 times with 1 × PBS. The cells were fixed and permeabilized using methanol, and stained with crystal violet. Colony formation rate = (number of cell colonies/number of seeded cells) × 100 %.

Subcutaneous Tumor-bearing Nude Mouse Experiment

Twelve 6-week-old male NSG mice were acquired from Vital River (https://vitalriver.biomart.cn/) and randomly divided into 3 groups, with 4 mice in each group. All mice were maintained in a specific pathogen-free (SPF) facility and were accommodated in colony cages at a temperature of 25°C, adhering to a 12-hour light/dark cycle, with ad libitum access to both food and water. WT and either MBNL1$^{-/-}$ or QKI$^{-/-}$ KYSE150 cells (2×10^6) in .1 mL of 1 × PBS were subcutaneously injected into the right flank of NSG mice, with the WT cell-injected group serving as the control. Tumor length (a) and width (b) were examined using vernier calipers every 4 days, beginning 14 days after implantation. Tumor volume was calculated using the formula: $1/2ab^2$. Thirty days after implantation, the mice were euthanized by asphyxiation using CO_2, and tumors were isolated and weighed. All data points are used for statistical analysis. The animal experiments in this study were done according to the approved protocol of the committee on animal care at the First Affiliated Hospital of Xinxiang Medical University (Approval number: 2018391) and adhered to the 'Guide for the Care and Use of Laboratory Animals, eighth Edition.[29] The reporting of this study conforms to ARRIVE 2.0 guidelines.[30]

Statistical Analysis

No specific statistical tests were employed to predetermine sample sizes. Statistical analyses were conducted in GraphPad Prism 7 software or SPSS version 23.0 (SPSS, Inc., IL). Data are presented as mean ± standard error of the mean (SEM). Differences between the 2 groups were examined using a Student's *t*-test. Kaplan-Meier analysis with a log-rank test was utilized for patient survival analysis. The correlation between MBNL1 or QKI expression and clinicopathological characteristics was examined using Pearson's χ^2 test. The difference was considered statistically significant when $P \leq .05$, while "ns" denotes no significance. *$P \leq .05$, **$P \leq .01$, ***$P \leq .001$, ****$P \leq .0001$.

Results

Correlation Between MBNL1 and QKI Expression with Prognosis of ESCC Patients

Prior studies demonstrated that MBNL1 and QKI display contrasting expression patterns across different tumor types.[11,14] To characterize their expression levels in ESCC, we utilized the GEO dataset GSE161533. The results revealed that both MBNL1 and QKI expression levels were significantly elevated in ESCC tissues relative to adjacent normal tissues (Figure 1(A) and (B)). In addition, immunohistochemistry (IHC) findings demonstrated that QKI expression substantially increased alongside the advancing TNM stage (Figure 1(D) and (F)), while MBNL1 expression maintained stability (Figure 1(C) and (E)).

Moreover, we assessed the links between MBNL1 or QKI expression and ESCC characteristics employing a tissue microarray containing 155 ESCC samples. IHC analysis suggested a correlation between high MBNL1 expression and patient age ($P < .05$), as well as between high QKI expression and tumor invasion depth ($P < .05$) (Table 1). However, Kaplan-Meier survival analysis unveiled no significant linkage between increased MBNL1 or QKI expression and poor prognosis in either EAC or ESCC ($P > .05$) (Figure 2(A)–(D)).

The Occurrence of ESCC Significantly Alters the Expression Levels of circRNA, lncRNA, and mRNA

To examine the influence of esophageal cancer on circRNA, lncRNA, and mRNA expression levels, we obtained clinical ESCC samples and matched normal tissue samples for RNA sequencing. The results demonstrated significant changes in circRNA expression in ESCC tissues relative to normal tissues, with 117 circRNAs noticeably reduced and 537 circRNAs markedly elevated (Figure 3(A) and (B)). We observed that 7 lncRNAs were significantly downregulated, while 110 lncRNAs were considerably upregulated (Figure 3(C) and (D)). Previous literature indicated that circRNA and lncRNA play crucial roles in regulating gene expression.[16] Correspondingly, we examined mRNA expression levels and uncovered that 16 genes were substantially suppressed, while 159 genes were conspicuously enhanced (Figure 3(E) and (F)). These findings suggested that ESCC development resulted in the upregulation of circRNA, lncRNA, and mRNA expression, which may rely on heightened MBNL1 and QKI expression levels.

Genetic Knockout of MBNL1 or QKI in KYSE150 ESCC Cells

MBNL1 and QKI have been identified as being essential for regulating circRNA production and tumor progression.[20] According to this understanding, producing MBNL1 or QKI knockout cell models could be invaluable for further mechanistic studies. Therefore, we employed CRISPR/Cas9 technology to knock out MBNL1 or QKI genes in KYSE150 cells. In our study, we designed 3 independent sgRNAs to remove exon 3 or exon 2 of MBNL1 or QKI, respectively (Supplemental Figure 1A and B). PCR screening and Sanger sequencing analyses revealed that significant deletions of DNA fragments occurred within the MBNL1 and QKI genes (Supplemental Figure 1C and D). In addition, qRT-PCR analysis indicated significant suppression of MBNL1 or QKI expression levels (Supplemental Figure 1E and F). Finally, western blot analysis suggested the complete knockout

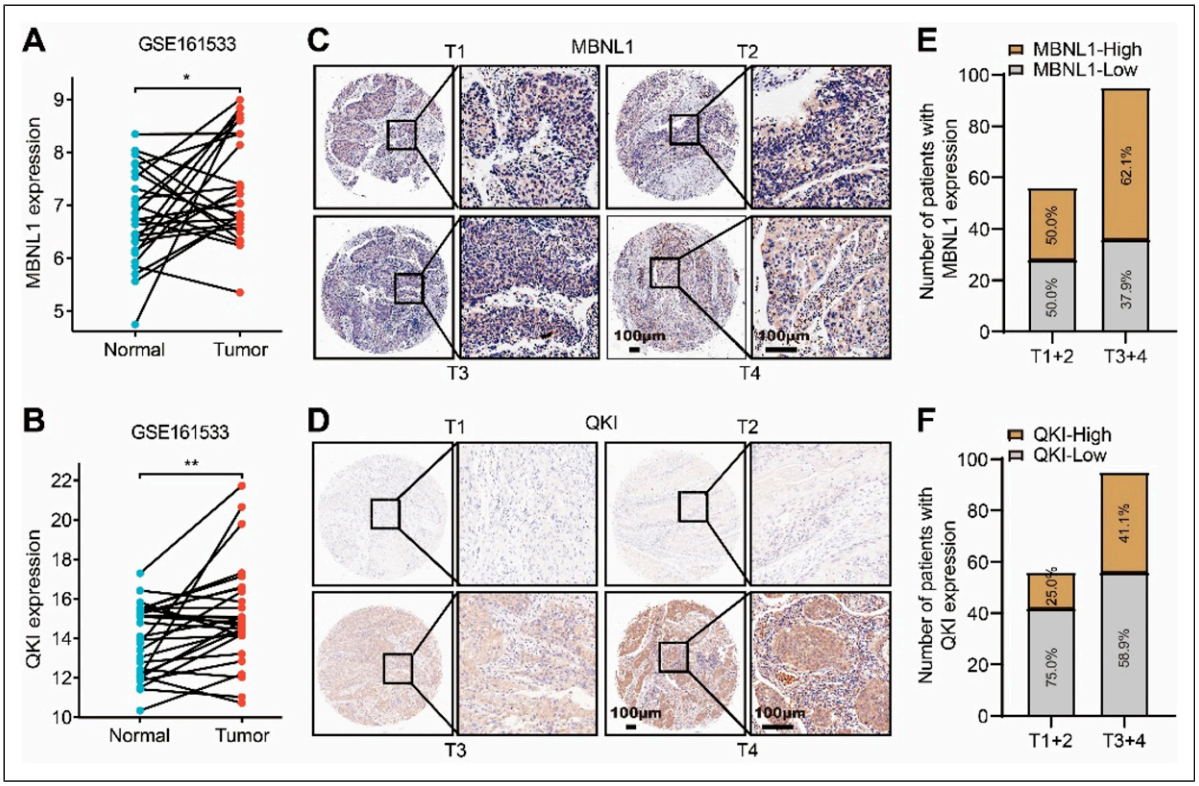

Figure 1. The expression of MBNL1 and QKI in human ESCC samples. (A) Expression patterns of MBNL1 in 28 ESCC as well as adjacent normal tissues according to GEO datasets. (B) Expression patterns of QKI in 28 ESCC and adjacent normal tissues according to GEO datasets. (C) IHC analysis of MBNL1 expression in various TNM stages of ESCC. (D) IHC analysis of QKI expression in various TNM stages of ESCC. (E and F) Bar chart of immunohistochemical staining scores for C and D. Data are presented as the mean ± SEM. $^{*}P < .05$, $^{**}P < .01$. Statistical significance was determined using an unpaired two-tailed Student's *t*-test.

of MBNL1 or QKI in KYSE150 cells (Supplemental Figure 1G). These results indicated the successful establishment of KYSE150 MBNL1$^{-/-}$ and QKI $^{-/-}$ cell lines.

MBNL1 or QKI Deficiency Dramatically Changes the Expression Levels of circRNA in ESCC Cells

RNA sequencing was performed to assess the influence of either MBNL1 or QKI on the expression levels of circRNA, lncRNA, and mRNA. As depicted in Figure 4(A) and (C), the ablation of MBNL1 in KYSE150 cells resulted in a significant increase in 189 circRNA expression levels and a notable decrease in the expression of 267 circRNAs. Additionally, QKI deficiency caused a significant increase in 43 circRNA expression levels and a pronounced decrease in 140 circRNA expression levels (Figure 4(B) and (D)). This data indicates that the knockout of either MBNL1 or QKI caused a larger portion of circRNAs to exhibit substantial downregulation. In addition, the circRNAs expressed as a consequence of MBNL1 or QKI knockout contain 61 shared circRNAs (Figure 4(E)). In Figure 4(F) and (G), the 20 most highly expressed circRNAs derived from MBNL1 or QKI deficiency are illustrated, with 3 circRNAs (hsa_circ_0125940, hsa_circ_0093201, and hsa_circ_0049133) being shared (Figure 4(H)).

Previous studies indicated that circRNAs can alter the stability of other RNA molecules, including lncRNAs and mRNAs.[31-34] Therefore, the expression levels of lncRNAs and mRNAs were examined and compared between the WT and MBNL1 or QKI-deficient KYSE150 cells through RNA sequencing. Intriguingly, substantial alterations were identified in the expression levels of numerous lncRNAs (Supplemental Figure 3A–D) and mRNAs (Figure 5(A)–(D)), with a higher proportion of genes exhibiting significant downregulation. Venn diagram analysis identified 84 mutually expressed lncRNAs (Supplemental Figure 3E) and 189 common mRNAs (Figure 5(E)), across both gene knockouts. Additionally, heatmap analysis of the top 20 differentially expressed lncRNAs and mRNAs uncovered 3 shared lncRNAs (URS0001BE5A8E, URS0001BF0B87, and URS0001D5898B, Supplemental Figure 3F–H) and 5 shared mRNAs (H2AC19, MAGEB2, SLCO4C1, TMPRSS15, and LOC102723728, Figure 5(F)–(H)). Except for H2AC19 and URS0001BF0B87, the expression patterns of the other

Table 1. Clinicopathological Correlation of MBNL1 and QKI Expression in ESCC.

		QKI Expression			MBNL1 Expression		
Clinical characteristics	Cases	Low Group(%)	High Group(%)	*P* Value	Low Group(%)	High Group(%)	*P* Value
Age(years old)							
≤60	52	31(59.6%)	21(40.4%)	0.3240	16(30.8%)	36(69.2%)	**0.0363**
>60	99	67(67.7%)	32(32.3%)		48(48.5%)	51(51.5%)	
Gender							
Male	97	63(64.9%)	34(35.1%)	0.9868	41(42.3%)	56(57.7%)	0.9691
Female	54	35(64.8%)	19(35.2%)		23(42.6%)	31(57.4%)	
Differentiation							
G1	78	53(67.9%)	35(32.1%)	0.1401	33(42.3%)	45(57.7%)	0.1765
G2	53	29(54.7%)	24(45.3%)		19(35.8%)	34(64.2%)	
G3	20	16(80.0%)	4(20.0%)		12(60.0%)	8(40.0%)	
Tumor invasion							
T1+T2	56	42(75.0%)	14(25.0%)	**0.0459**	28(50.0%)	28(50.0%)	0.1459
T3+T4	95	56(58.9%)	39(41.1%)		36(37.9%)	59(62.1%)	
Lymph node metastasis							
N0	106	66(62.3%)	40(37.7%)	0.2975	46(43.4%)	60(56.6%)	0.6993
N1	45	32(71.1%)	13(28.9%)		18(40.0%)	27(60.0%)	
Distant metastasis							
M0	133	88(66.2%)	45(33.8%)	0.3761	59(44.4%)	74(55.6%)	0.1815
M1	18	10(55.6%)	8(44.4%)		5(27.8%)	13(72.2%)	
Clinical stage							
Early (I- II)	99	63(63.6%)	36(36.4%)	0.6533	45(45.5%)	54(54.5%)	0.2921
Advanced (III - IV)	52	35(67.3%)	17(32.7%)		19(36.5%)	33(63.5%)	

Statistical significance ($p < 0.05$) is shown in bold.

6 genes were verified using qRT-PCR, which is consistent with the RNA-seq results (Figure 5(I), Supplemental Figure 3I). Moreover, we mapped differentially expressed mRNAs to the KEGG databases to identify the signaling pathways influenced by the absence of MBNL1 or QKI in KYSE150 cells. The most significantly perturbed pathways are illustrated in Supplemental Figure 2, underscoring the top 20 enriched pathways. KEGG pathway analysis uncovered that lacking MBNL1 influenced several critical pathways linked to tumor progression, such as the cell cycle, p53 signaling pathway, cellular senescence, the FoxO signaling pathway, and apoptosis. Similarly, the loss of QKI impacted the cell cycle and p53 signaling pathway, suggesting a potential overlap in the molecular outcomes of MBNL1 and QKI deficiencies. Consequently, this strongly suggests that the deficiency of either MBNL1 or QKI causes substantial alterations in the expression levels of circRNA, lncRNA, and mRNA in KYSE150 cells, potentially impacting tumor progression.

Depletion of MBNL1 or QKI Improves the Migration, Invasion, and Proliferation Abilities of KYSE150 Cells

The successful production of KYSE150 cells deficient in MBNL1 or QKI facilitated the comprehensive assessment of phenotypic alterations in cells without MBNL1 or QKI. Deficient and control cells were seeded into upper chambers with or without Matrigel coating for a Transwell assay, or into 12 well plates containing 500 cells per well for colony formation assay. Remarkably, Transwell assays suggested that the knockout of either MBNL1 or QKI significantly enhanced the migratory and invasive capacities in KYSE150 cell models (Figure 6(A)–(D)). Cell growth assays identified that cells lacking MBNL1 or QKI notably improved colony formation capacity compared to WT KYSE150 cells (Figure 6(E) and (F)). These findings indicate that both MBNL1 and QKI are tumor suppressors in KYSE150 cells.

Absence of MBNL1 or QKI Promotes Tumor Growth of ESCC in Xenograft Model

To examine the role of MBNL1 or QKI in regulating tumor growth in vivo, we subcutaneously injected mice with KYSE150 cells. The findings revealed that knockouts of MBNL1 or QKI significantly increased the subcutaneous tumorigenesis of esophageal cancer cells. Notably, a statistically significant elevation in tumor volume was identified in the $MBNL1^{-/-}$ and $QKI^{-/-}$ groups relative to the control group (Figure 7(A) and (B)). In addition, the tumor weight in the $MBNL1^{-/-}$ and $QKI^{-/-}$ groups significantly increased compared to the WT control group (Figure 7(C)–

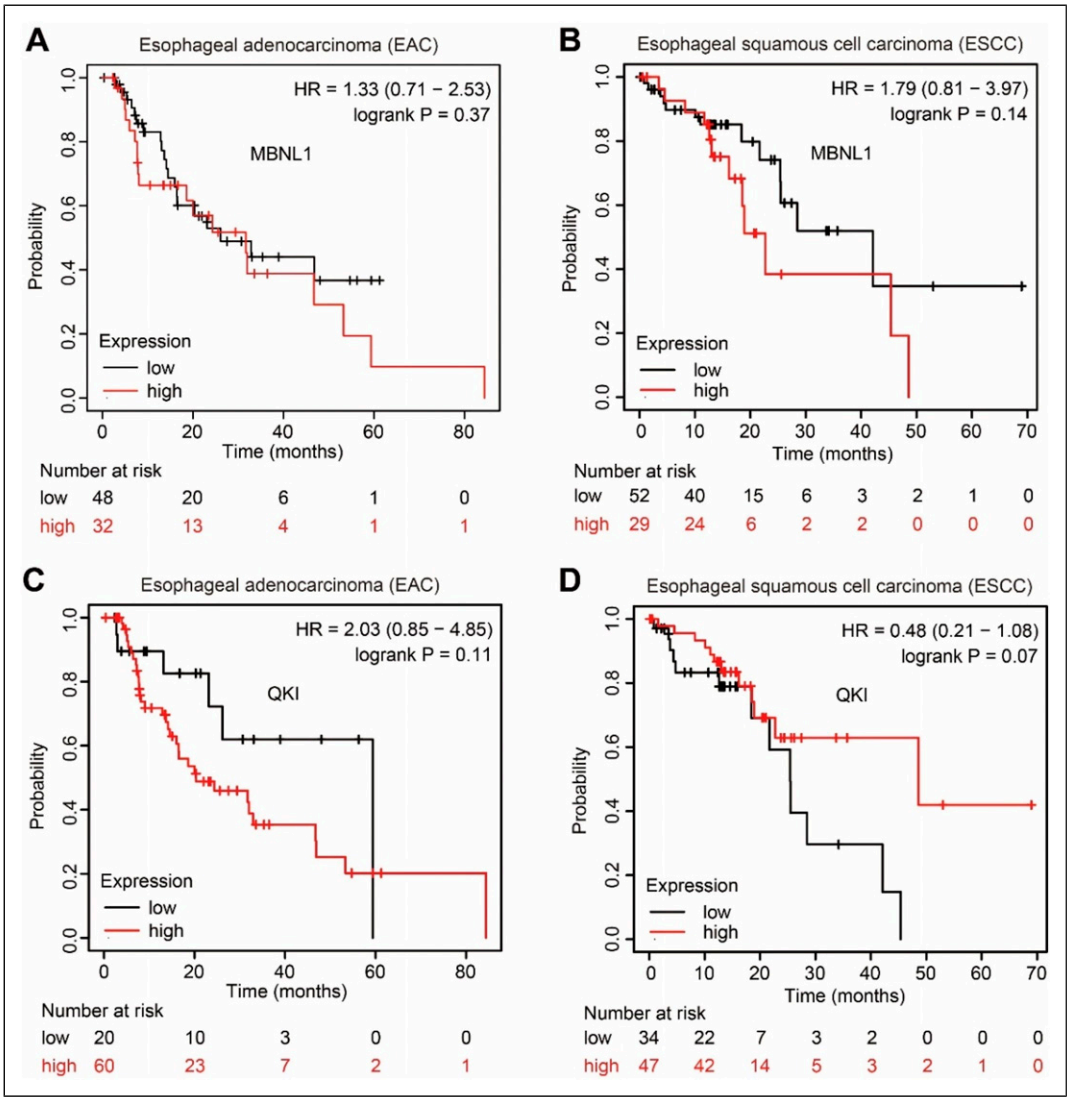

Figure 2. Kaplan-Meier survival analysis between the expression of MBNL1 or QKI and poor prognosis of EAC or ESCC patients. (A) Correlation examination between the expression of MBNL1 and the poor prognosis of EAC patients. (B) Correlation analysis between the expression of MBNL1 and the poor prognosis of ESCC patients. (C) Correlation analysis between the expression of QKI and the poor prognosis of EAC patients. (D) Correlation analysis between the expression of QKI and the poor prognosis of ESCC patients.

(E)). These findings provide compelling evidence that the MBNL1 and QKI genes are important for inhibiting tumor growth.

Discussion

In this study, we identified that 2 RNA-binding proteins, MBNL1 and QKI, functioning as pre-mRNA alternative splicing regulators of circRNAs, are abundantly expressed throughout ESCC in human patients. While high MBNL1 or QKI expression was not significantly associated with negative prognosis in patients with EAC or ESCC, their expression levels were significantly elevated in human ESCC tumor tissue compared to normal tissues. The molecular mechanism behind the upregulation of MBNL1 and QKI expression remains unclear. We hypothesize that ESCC development may influence the expression levels of these 2 genes in diverse ways, such as altering the function of transcription factors that modulate their expression levels.

Interestingly, increased MBNL1 expression is significantly correlated with patient age, while high QKI expression is linked to tumor invasion, indicating distinct roles for these 2 proteins. Unexpectedly, when conducting CRISPR/Cas9-mediated knockout of these 2 proteins in ESCC cells, we determined that the absence of MBNL1 or QKI in KYSE150 ESCC cells substantially improved cell migration, invasion, and proliferation. We identified elevated levels of MBNL1 and QKI in tumor tissues, while the absence of their

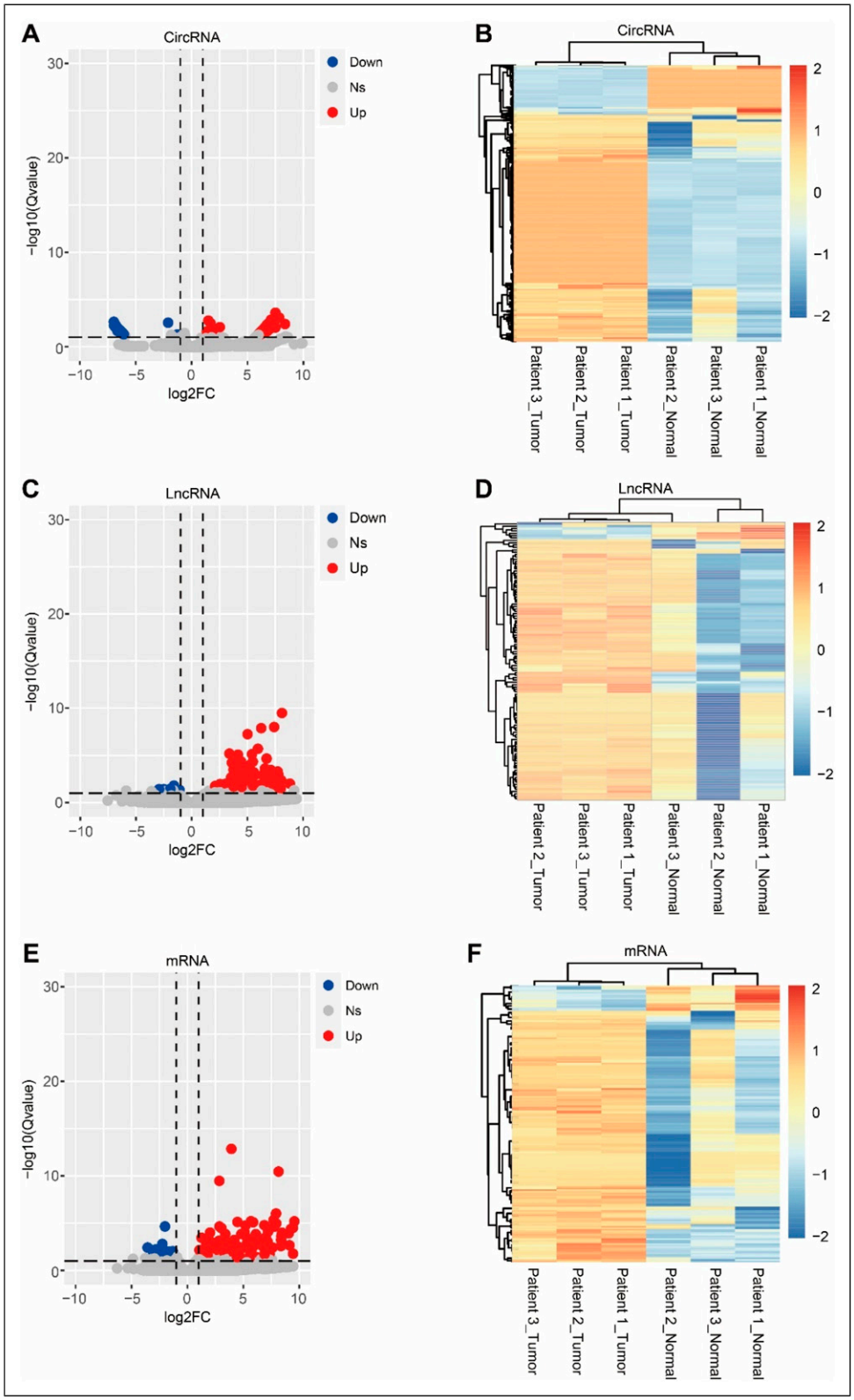

Figure 3. The occurrence of ESCC significantly influenced the expression patterns of circRNA, lncRNA, and mRNA species. (A) Volcano plot indicating the expression differences of circRNAs between ESCC and adjacent normal tissues. Blue dots depict downregulated genes. Red dots represent upregulated genes. (B) Heatmap of differentially expressed circRNAs across ESCC and adjacent normal tissues. (C) Volcano plot illustrating the expression differences of lncRNAs between ESCC and adjacent normal tissues. (D) Heatmap of differentially expressed lncRNAs throughout ESCC and adjacent normal tissues. (E) Volcano plot presenting the expression differences of mRNAs between ESCC and adjacent normal tissues. (F) Heatmap of differentially expressed mRNAs across ESCC and adjacent normal tissues.

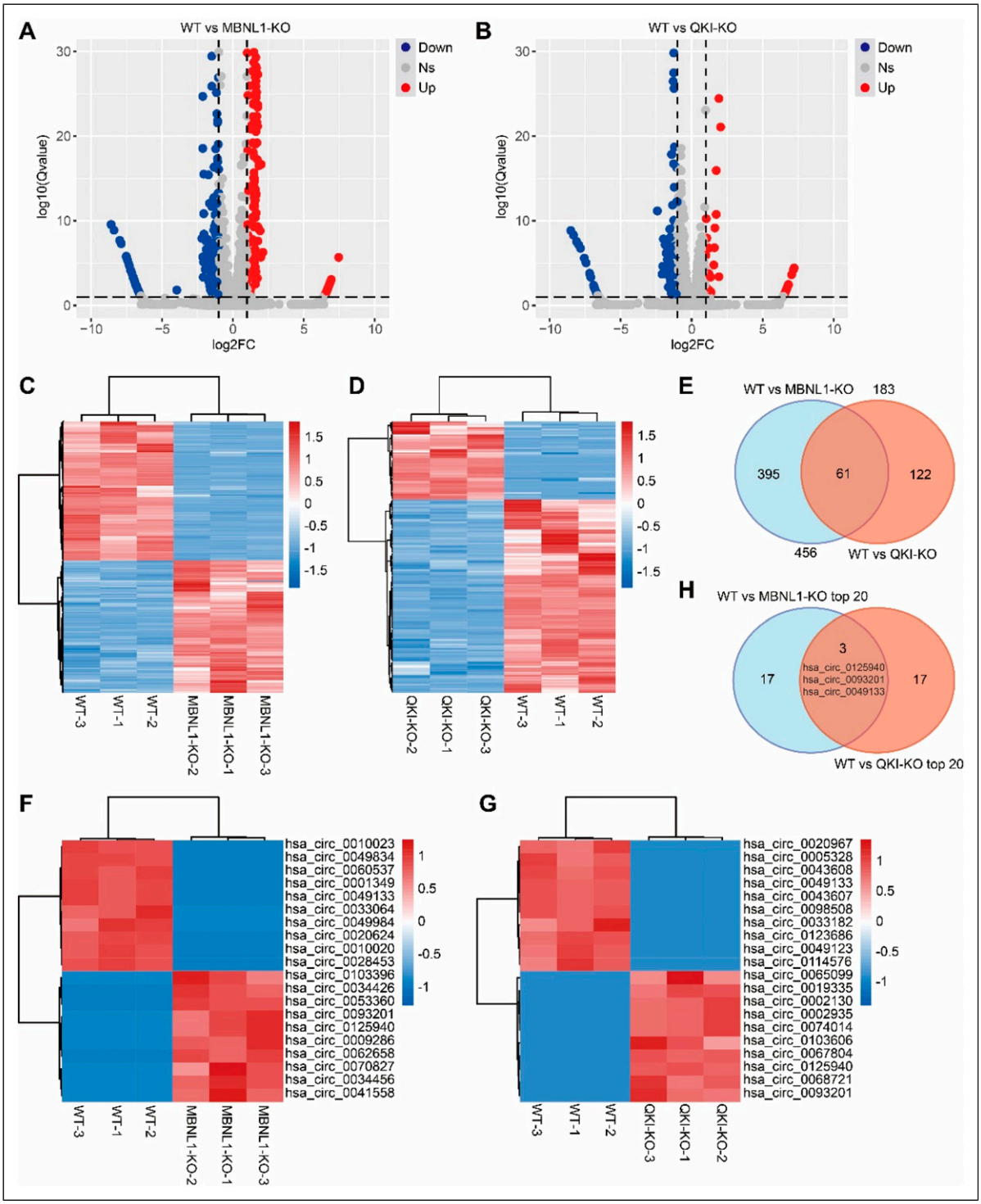

Figure 4. Influence of MBNL1 or QKI-deficiency on the expression patterns of circRNAs. (A and B) Volcano plot depicting the expression differences of circRNAs between WT and MBNL1 (A) or QKI (B)-deficient KYSE150 cells. Blue dots indicate downregulated genes. Red dots indicate upregulated genes. (C and D) Heatmap of differentially expressed circRNAs between WT and MBNL1 (C) or QKI (D)-deficient KYSE150 cells. (E) Venn diagram analysis of differentially expressed circRNAs between MBNL1$^{-/-}$ and QKI$^{-/-}$ KYSE150 cells. (F and G) Heatmap displaying the top 20 differentially expressed circRNAs between WT and MBNL1 (F) or QKI (G)-deficient KYSE150 cells. (H) Venn diagram analysis of the top 20 differentially expressed circRNAs across MBNL1$^{-/-}$ and QKI$^{-/-}$ KYSE150 cells.

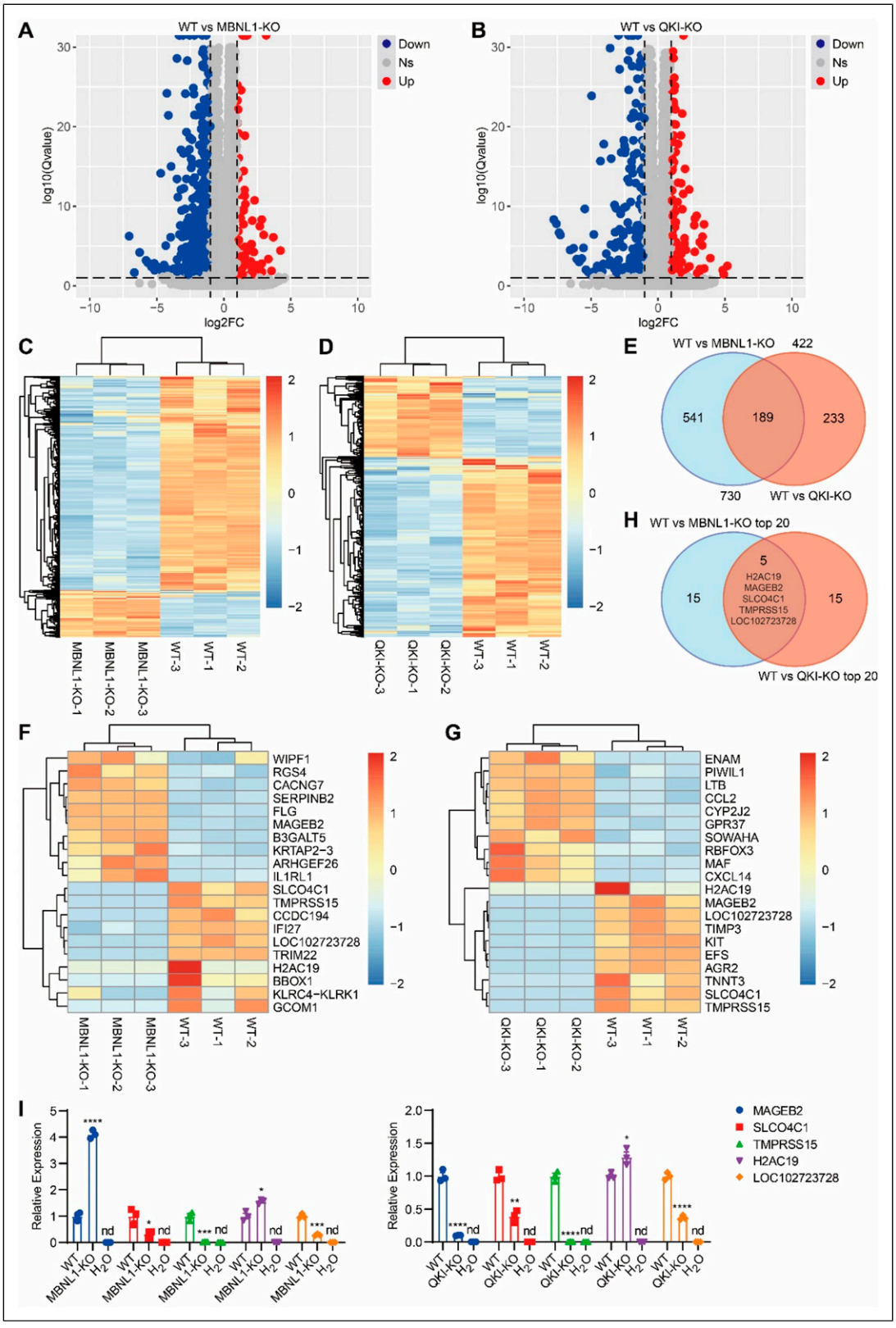

Figure 5. Impact of MBNL1 or QKI-deficiency on the expression patterns of mRNAs. (A and B) Volcano plot illustrating the expression differences of mRNAs between WT and MBNL1 (A) or QKI (B)-deficient KYSE150 cells. Blue dots depict downregulated genes. Red dots indicate upregulated genes. (C and D) Heatmap of differentially expressed mRNAs across WT and MBNL1 (C) or QKI (D)-deficient KYSE150 cells. (E) Venn diagram analysis of differentially expressed mRNAs across MBNL1$^{-/-}$ and QKI$^{-/-}$ KYSE150 cells. (F and G) Heatmap displaying the top 20 differentially expressed mRNAs between WT and MBNL1 (F) or QKI (G)-deficient KYSE150 cells. (H) Venn diagram assessment of the top 20 differentially expressed mRNAs between MBNL1$^{-/-}$ and QKI$^{-/-}$ KYSE150 cells. (I) qRT-PCR confirmed 5 overlapping mRNAs in the top 20 differentially expressed genes between MBNL1$^{-/-}$ and QKI$^{-/-}$ KYSE150 cells. WT was the positive control, and H_2O was the negative control. nd = not detected. This experiment was performed 3 times independently, and the data are presented as the mean ± SEM. *$P < .05$, **$P < .01$, ***$P < .001$, ****$P < .0001$. Statistical significance was determined using an unpaired two-tailed Student's *t*-test.

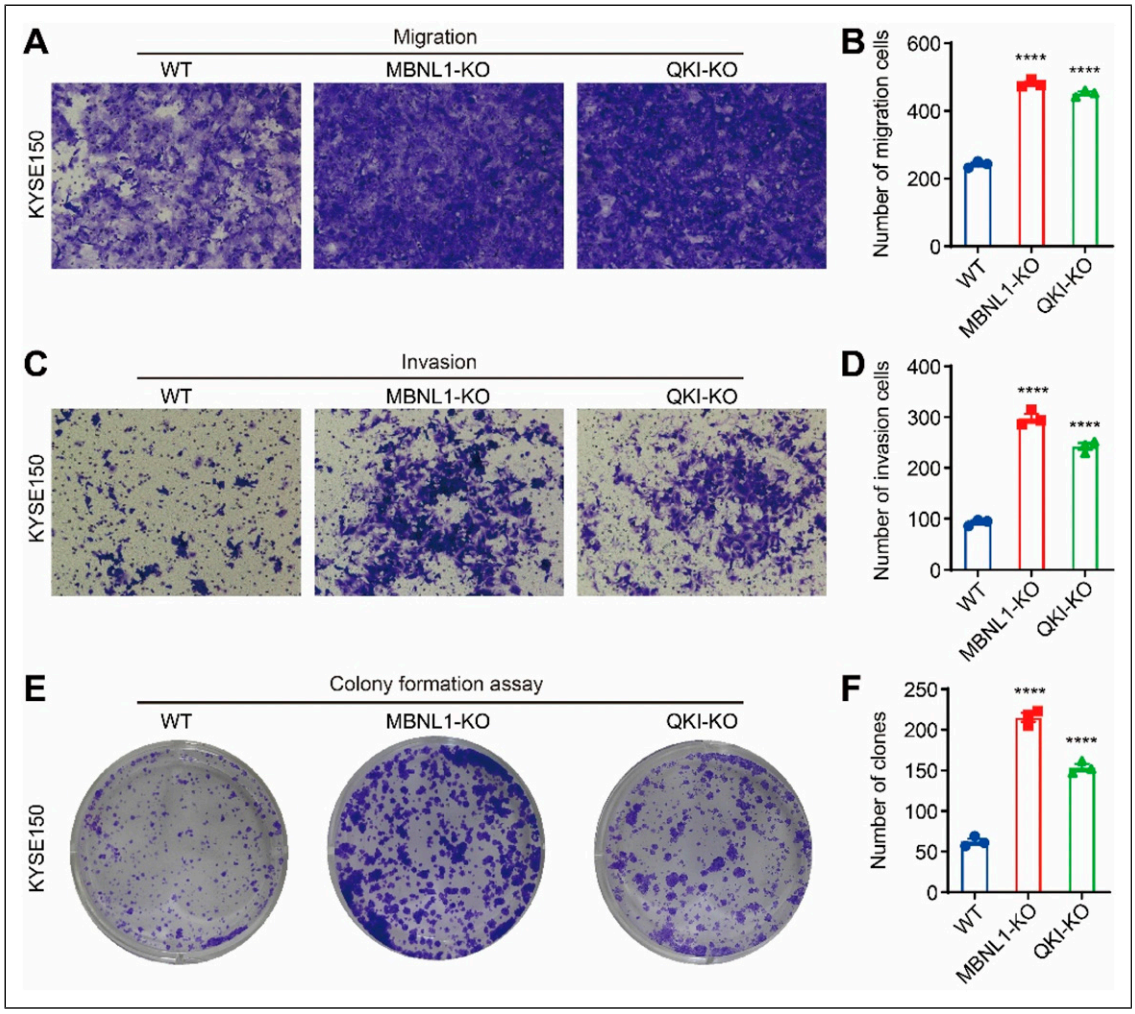

Figure 6. Depletion of MBNL1 or QKI improves the migration, invasion, and proliferation abilities of KYSE150 cells. (A) Transwell assay indicating that knockout of MBNL1 or QKI improved cell migration in KYSE150 cells. This experiment was repeated 3 times independently. (B) Quantification of (A). (C) Transwell assay demonstrating that knockout of MBNL1 or QKI improved cell invasion in KYSE150 cells. This experiment was repeated 3 times independently. (D) Quantification of (C). (E) Colony formation assay indicating that knockout of MBNL1 or QKI enhanced cell proliferation in KYSE150 cells. This experiment was repeated 3 times independently. (F) Quantification of (E). Data are presented as the mean ± SEM. ****$P < .0001$. Statistical significance was determined using an unpaired two-tailed Student's *t*-test.

expression in ESCC cells promoted cell migration, invasion, and proliferation. This indicated that the upregulation of MBNL1 or QKI in tumor tissue was a negative feedback mechanism to inhibit ESCC. Genetic evidence supports the role of MBNL1 and QKI as tumor suppressors in ESCC. According to these findings, we suggest that tuning MBNL1 or QKI expression may represent a potential strategy for ESCC treatment.

CircRNAs represent endogenous RNAs created through a specific back-splicing mechanism designated for pre-mRNAs. They can be classified into 3 groups according to their composition: exon circRNAs (EcircRNAs), circular intronic RNAs (ciRNAs), and Exon-Intron circRNAs (EIciRNAs).[35] The circulation of EIciRNA and EcircRNA is usually spearheaded by intron pairing, RBPs, or lariats.[36-39] Two key RBPs, MBNL1 and QKI, regulate circRNA production and are pivotal players in assorted tumors. Earlier research has indicated that QKI expression in lung cancer is markedly lower than in normal tissues, associated with poorer patient prognosis.[40-42] Furthermore, QKI in normal cells selectively limits the splicing of exon 12 of NUMB mRNA by competing with the core splicing factor SF1, elevating the expression level of NUMB isoforms, hindering cell proliferation, and halting the activation of the Notch signaling pathway.[12,43] Conversely, MBNL1 reinforces stability in breast cancer by attaching to the 3' untranslated region (3' UTR) of DBNL (Drebrin-like protein) and TACC1 (transforming acid spiral protein 1) transcripts, impeding the invasion of breast cancer cells.[44] In addition, MBNL1 is a suppressor of tumor dedifferentiation, with research revealing that a reduction in

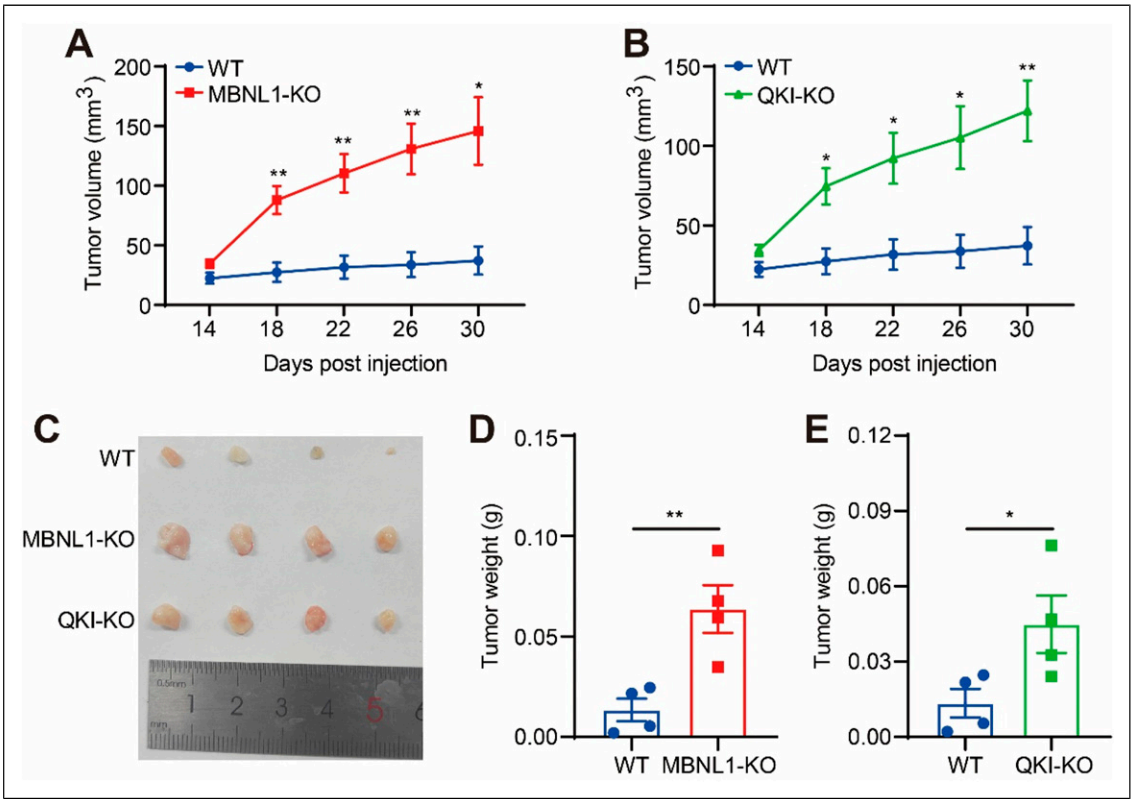

Figure 7. The absence of MBNL1 or QKI promotes tumor growth of ESCC in xenograft models. (A) Tumor growth in NSG mice subcutaneously inoculated with KYSE150 WT and MBNL1$^{-/-}$ KYSE150 cells (n = 4). (B) Tumor growth in NSG mice subcutaneously inoculated with KYSE150 WT and QKI$^{-/-}$ KYSE150 cells (n = 4). (C–E) Tumor image (C), and tumor weight (D and E) in NSG mice subcutaneously inoculated with KYSE150 WT, MBNL1$^{-/-}$ and QKI$^{-/-}$ KYSE150 cells (n = 4). Data are presented as the mean ± SEM. *P < .05, **P < .01. Statistical significance was determined using an unpaired two-tailed Student's t-test.

MBNL1 expression signals poor survival rates in lung, breast, and stomach adenocarcinomas alongside increased recurrence and metastasis in breast cancer.[45] Additionally, reduced MBNL1 expression accelerates tumor progression in vitro and in vivo.[45] Interestingly, MBNL1 can behave as an effective inhibitor of CRC cell metastasis by modulating the expression of miR-1307 as well as its target gene, Bcl2.[46]

Our study highlighted that both MBNL1 and QKI are suppressors in ESCC (Figure 6, Figure 7). Moreover, our study determined that the depletion of MBNL1 or QKI in KYSE150 cells leads to substantial alterations in the expression profiles of various circRNAs (Figure 4). This observation suggests a role for MBNL1 and QKI in the circRNA production in KYSE150 cells. Intriguingly, recent studies have found that circRNAs can influence the stability of other RNA species, including lncRNAs and mRNAs.[31-34] Corroborating these findings, we found notable differences in the expression levels of lncRNAs and mRNAs during MBNL1 or QKI depletion in KYSE150 cells (Supplemental Figure 3, Figure 5). This suggests a potential cascade in which the loss of MBNL1 and QKI initially modulates circRNA expression, governing the stability and the abundance of downstream lncRNAs and mRNAs. However, as contrasted with the knockout of an individual gene, we hypothesize that simultaneously knocking out both MBNL1 and QKI genes in KYSE150 cells exerts distinct effects on the expression levels of circRNA, lncRNA, and mRNA. After the knockout of either MBNL1 or QKI, multiple overlapping genes were found, ranging from dozens to hundreds, among the differential expression of circRNA, lncRNA, and mRNA species (Figure 4(E), Supplemental Figure 3E, Figure 5(E)). Notably, several overlapping genes were identified between the top 20 differentially expressed genes in MBNL1 and QKI-deficient cells (Figure 4(F), Supplemental Figure 3F, Figure 5(F)). Nonetheless, the functions of overlapping circRNAs (hsa_circ_0125940, hsa_circ_0093201, and hsa_circ_0049133) and lncRNAs (URS0001BE5A8E and URS0000D5898B) remain unreported. Notably, among the 4 differentially expressed mRNAs, the expression levels of SLCO4C1, TMPRSS15, and LOC102723728 were lowered in MBNL1 or QKI knockout KYSE150 cells, while MAGEB2 expression dropped in QKI-deficient cells while it surged in MBNL1-deficient cells.

Prior studies have confirmed that SLCO4C1 has relatively low expression in prostate cancer,[47] acting as a protective gene for patient prognosis in colon adenocarcinoma.[48] Another

study proposed a significant association between the expression of TMPRSS15 and patient prognosis in gastric cancer.[49] Our research findings mirror these findings. Conversely, it has been reported that the human MAGEB2 protein enhances E2F transcription factor activity through interaction with HDAC, triggering the proliferation of HCT116 and U2OS cells.[50] Similarly, the upregulation of MAGEB2 expression in laryngeal cancer cells has been linked to increased cell proliferation, migration, and invasion.[51] These findings are aligned with our results pertaining to cells deficient in MBNL1, but contradict our findings in cells deficient in QKI. However, the influence and roles of SLCO4C1, TMPRSS15, MAGEB2, and LOC102723728 in the progression of ESCC were not identified in this study, necessitating further investigation.

The limitations of the current study include the absence of normal esophageal tissue collection during the sampling process; we solely harvested cancerous tissues from patients with various stages of ESCC, which were subsequently utilized for IHC assays. Additionally, we deployed RNA sequencing to screen for circRNAs, lncRNAs, and mRNAs in KYSE150 cells that demonstrated considerable alterations in expression levels post-knockout of MBNL1 or QKI. However, these differentially expressed genes require further analysis to confirm their functions.

Conclusion

In conclusion, our study affirms prior results that attributed tumor-suppressing functionality to MBNL1 and QKI in experimental studies of ESCC. We uncovered that depletion of either MBNL1 or QKI exacerbated ESCC cell migration, invasion, and proliferation by altering various circRNA, lncRNA, and mRNA expression patterns. Consequently, MBNL1 and QKI could serve as diagnostic biomarkers and therapeutic targets for the treatment of ESCC.

Author Contributions

Conceptualization and supervision, Yulong Liu and Xiumin Li; Methodology, Haifeng Wang, Xiaofeng Zhou, Jinghan Hou, Qunmei Zhang, Jieqing Wu, and Xuelian Xu; Validation, Yulong Liu; Review and editing, Yulong Liu; Funding acquisition, Yulong Liu. All authors have read and agreed to the published version of the manuscript.

Acknowledgments

The authors would like to thank the staff of the Laboratory of Mouse Genetics at Xinxiang Medical University for their help and technical assistance.

Declaration of Conflicting Interests

The author(s) declared no potential conflicts of interest with respect to the research, authorship, and/or publication of this article.

Funding

The author(s) disclosed receipt of the following financial support for the research, authorship, and/or publication of this article: This work was supported by the Discipline Construction Promotion Project of the Second Affiliated Hospital of Soochow University (a team project of application innovation of nuclear technology in medicine) (serial number: XKTJHTD2021001) & the Priority Academic Program Development of Jiangsu Higher Education Institutions (PAPD).

Ethical Statement

Ethical Approval

The Ethics Committee of the First Affiliated Hospital of Xinxiang Medical University approved the ESCC samples used in this study (ethics approval number: 2018390), and all experiments were conducted in strict compliance with the Declaration of Helsinki.

Informed Consent

All participants signed an informed consent form. The animal experiments in this study were done according to the approved protocol of the committee on animal care at the First Affiliated Hospital of Xinxiang Medical University (Approval number: 2018391) and adhered to the 'Guide for the Care and Use of Laboratory Animals, eighth Edition.

ORCID iDs

Jing-Han Hou https://orcid.org/0009-0009-9944-4122
Yu-Long Liu https://orcid.org/0000-0003-2660-8076

Data Availability Statement

All data needed to evaluate the conclusions in the paper are present in the paper and/or the Supplementary Materials. The datasets used and/or analyzed during the current study are available from the corresponding author upon reasonable request.

Supplemental Material

Supplemental material for this article is available online.

References

1. Sung H, Ferlay J, Siegel RL, et al. Global Cancer Statistics 2020: GLOBOCAN Estimates of incidence and mortality worldwide for 36 cancers in 185 countries. *CA Cancer J Clin*. 2021;71(3):209-249.
2. Zhang X, Wang YX, Meng LH. Comparative genomic analysis of esophageal squamous cell carcinoma and adenocarcinoma: new opportunities towards molecularly targeted therapy. *Acta Pharm Sin B*. 2022;12(3):1054-1067.
3. Rogers JE, Sewastjanow-Silva M, Waters RE, Ajani JA. Esophageal cancer: emerging therapeutics. *Expert Opin Ther Targets*. 2022;26(2):107-117.

4. DiSiena M, Perelman A, Birk J, Rezaizadeh H. Esophageal cancer: an updated review. *South Med J*. 2021;114(3):161-168.
5. Yu CP, Chen K, Zheng HQ, et al. Overexpression of astrocyte elevated gene-1 (AEG-1) is associated with esophageal squamous cell carcinoma (ESCC) progression and pathogenesis. *Carcinogenesis*. 2009;30(5):894-901.
6. Yang CC, Zheng ST, Liu Q, et al. Metadherin is required for the proliferation, migration, and invasion of esophageal squamous cell carcinoma and its meta-analysis. *Transl Res*. 2015;166(6): 614-626.e612.
7. Ma S, Lu CC, Yang LY, et al. ANXA2 promotes esophageal cancer progression by activating MYC-HIF1A-VEGF axis. *J Exp Clin Cancer Res*. 2018;37(1):183.
8. Li YJ, Yang Q, Chen H, et al. TFAM downregulation promotes autophagy and ESCC survival through mtDNA stress-mediated STING pathway. *Oncogene*. 2022;41(30):3735-3746.
9. Liu WL, Miao CW, Zhang SS, et al. VAV2 is required for DNA repair and implicated in cancer radiotherapy resistance. *Signal Transduct Target Ther*. 2021;6(1):322.
10. Chen YZ, Wang DD, Peng H, et al. Epigenetically upregulated oncoprotein PLCE1 drives esophageal carcinoma angiogenesis and proliferation via activating the PI-PLCepsilon-NF-kappaB signaling pathway and VEGF-C/Bcl-2 expression. *Mol Cancer*. 2019;18(1):1.
11. Zhang Q, Wu YX, Chen JL, et al. The regulatory role of both MBNL1 and MBNL1-AS1 in several common cancers. *Curr Pharm Des*. 2022;28(7):581-585.
12. Coomer AO, Black F, Greystoke A, et al. Alternative splicing in lung cancer. *Biochim Biophys Acta Gene Regul Mech*. 2019; 1862(11-12):194388.
13. Yang GD, Fu HY, Zhang J, et al. RNA-binding protein quaking, a critical regulator of colon epithelial differentiation and a suppressor of colon cancer. *Gastroenterology*. 2010;138(1): 231.e231.
14. Bian YQ, Wang L, Lu HY, et al. Downregulation of tumor suppressor QKI in gastric cancer and its implication in cancer prognosis. *Biochem Biophys Res Commun*. 2012;422(1): 187-193.
15. Zhao Y, Zhang G, Wei MY, et al. The tumor suppressing effects of QKI-5 in prostate cancer: a novel diagnostic and prognostic protein. *Cancer Biol Ther*. 2014;15(1):108-118.
16. Bandopadhayay P, Ramkissoon LA, Jain P, et al. MYB-QKI rearrangements in angiocentric glioma drive tumorigenicity through a tripartite mechanism. *Nat Genet*. 2016;48(3):273-282.
17. Dhaenens CM, Schraen-Maschke S, Tran H, et al. Overexpression of MBNL1 fetal isoforms and modified splicing of Tau in the DM1 brain: two individual consequences of CUG trinucleotide repeats. *Exp Neurol*. 2008;210(2):467-478.
18. Kristensen LS, Andersen MS, Stagsted LVW, et al. The biogenesis, biology and characterization of circular RNAs. *Nat Rev Genet*. 2019;20(11):675-691.
19. Danan-Gotthold M, Golan-Gerstl R, Eisenberg E, et al. Identification of recurrent regulated alternative splicing events across human solid tumors. *Nucleic Acids Res*. 2015;43(10): 5130-5144.
20. Li X, Yang L, Chen LL. The biogenesis, functions, and challenges of circular RNAs. *Mol Cell*. 2018;71(3):428-442.
21. Chen L, Shan G. CircRNA in cancer: fundamental mechanism and clinical potential. *Cancer Lett*. 2021;505:49-57.
22. Luo J, Lu LX, Gu YR, et al. Speed genome editing by transient CRISPR/Cas9 targeting and large DNA fragment deletion. *J Biotechnol*. 2018;281:11-20.
23. Li RQ, Li YR, Kristiansen K, Wang J. SOAP: short oligonucleotide alignment program. *Bioinformatics*. 2008;24(5): 713-714.
24. Kim D, Langmead B, Salzberg SL. HISAT: a fast spliced aligner with low memory requirements. *Nat Methods*. 2015;12(4): 357-360.
25. Langmead B, Salzberg SL. Fast gapped-read alignment with Bowtie 2. *Nat Methods*. 2012;9(4):357-359.
26. Li B, Dewey CN. RSEM: accurate transcript quantification from RNA-Seq data with or without a reference genome. *BMC Bioinform*. 2011;12:323.
27. Love MI, Huber W, Anders S. Moderated estimation of fold change and dispersion for RNA-seq data with DESeq2. *Genome Biol*. 2014;15(12):550.
28. Zhou XF, Li YJ, Wang WL, et al. Regulation of Hippo/YAP signaling and esophageal squamous carcinoma progression by an E3 ubiquitin ligase PARK2. *Theranostics*. 2020;10(21): 9443-9457.
29. National Research Council (US). Committee for the update of the guide for the care and use of laboratory animals. In: *Guide for the Care and Use of Laboratory Animals*. 8th ed. Washington (DC): National Academies Press (US); 2011.
30. Percie du Sert N, Hurst V, Ahluwalia A, et al. The ARRIVE guidelines 2.0: updated guidelines for reporting animal research. *Br J Pharmacol*. 2020;177(16):3617-3624.
31. Pisignano G, Michael DC, Visal TH, et al. Going circular: history, present, and future of circRNAs in cancer. *Oncogene*. 2023;42(38):2783-2800.
32. Hansen TB, Wiklund ED, Bramsen JB, et al. miRNA-dependent gene silencing involving Ago2-mediated cleavage of a circular antisense RNA. *EMBO J*. 2011;30(21): 4414-4422.
33. Chen R-X, Chen X, Xia L-P, et al. N6-methyladenosine modification of circNSUN2 facilitates cytoplasmic export and stabilizes HMGA2 to promote colorectal liver metastasis. *Nat Commun*. 2019;10(1):4695.
34. Rossi F, Beltran M, Damizia M, et al. Circular RNA ZNF609/CKAP5 mRNA interaction regulates microtubule dynamics and tumorigenicity. *Mol Cell*. 2022;82(1):75-89.e79.
35. Gao Y, Wang JF, Zheng Y, et al. Comprehensive identification of internal structure and alternative splicing events in circular RNAs. *Nat Commun*. 2016;7:12060.
36. Eger N, Schoppe L, Schuster S, et al. Circular RNA splicing. *Adv Exp Med Biol*. 2018:41-52.
37. Conn SJ, Pillman KA, Toubia J, et al. The RNA binding protein quaking regulates formation of circRNAs. *Cell*. 2015;160(6): 1125-1134.

38. Petkovic S, Muller S. RNA circularization strategies in vivo and in vitro. *Nucleic Acids Res*. 2015;43(4):2454-2465.
39. Zheng SL, Zhang XJ, Odame E, et al. CircRNA-Protein interactions in muscle development and diseases. *Int J Mol Sci*. 2021;22(6):3262.
40. Kim EJ, Kim JS, Lee S, et al. QKI, a miR-200 target gene, suppresses epithelial-to-mesenchymal transition and tumor growth. *Int J Cancer*. 2019;145(6):1585-1595.
41. de Miguel FJ, Pajares MJ, Martinez-Terroba E, et al. A large-scale analysis of alternative splicing reveals a key role of QKI in lung cancer. *Mol Oncol*. 2016;10(9):1437-1449.
42. Liang G, Meng W, Huang XJ, et al. miR-196b-5p-mediated downregulation of TSPAN12 and GATA6 promotes tumor progression in non-small cell lung cancer. *Proc Natl Acad Sci U S A*. 2020;117(8):4347-4357.
43. Zong FY, Fu X, Wei WJ, et al. The RNA-binding protein QKI suppresses cancer-associated aberrant splicing. *PLoS Genet*. 2014;10(4):e1004289.
44. Fish L, Pencheva N, Goodarzi H, et al. Muscleblind-like 1 suppresses breast cancer metastatic colonization and stabilizes metastasis suppressor transcripts. *Genes Dev*. 2016;30(4):386-398.
45. Ray D, Yun YC, Idris M, et al. A tumor-associated splice-isoform of MAP2K7 drives dedifferentiation in MBNL1-low cancers via JNK activation. *Proc Natl Acad Sci U S A*. 2020; 117(28):16391-16400.
46. Tang R, Qi QH, Wu RR, et al. The polymorphic terminal-loop of pre-miR-1307 binding with MBNL1 contributes to colorectal carcinogenesis via interference with Dicer1 recruitment. *Carcinogenesis*. 2015;36(8):867-875.
47. Li X, Zhang WF, Song J, et al. SLCO4C1 promoter methylation is a potential biomarker for prognosis associated with biochemical recurrence-free survival after radical prostatectomy. *Clin Epigenetics*. 2019;11(1):99.
48. Zhu LY, Sun HY, Tian G, et al. Development and validation of a risk prediction model and nomogram for colon adenocarcinoma based on methylation-driven genes. *Aging (Albany NY)*. 2021; 13(12):16600-16619.
49. Wei XJ, Liu J, Hong ZJ, et al. Identification of novel tumor microenvironment-associated genes in gastric cancer based on single-cell RNA-sequencing datasets. *Front Genet*. 2022;13: 896064.
50. Peche LY, Ladelfa MF, Toledo MF, et al. Human MageB2 protein expression enhances E2F transcriptional activity, cell proliferation, and resistance to ribotoxic stress. *J Biol Chem*. 2015;290(49):29652-29662.
51. Cui J, Chen YS, Ou YP, et al. Cancer germline antigen gene MAGEB2 promotes cell invasion and correlates with immune microenvironment and immunotherapeutic efficiency in laryngeal cancer. *Clin Immunol*. 2022;240: 109045.